Available online at www.sciencedirect.com
SCIENCE DIRECT®
Journal of Sound and Vibration 276 (2004) 627–648
JOURNAL OF SOUND AND VIBRATION
www.elsevier.com/locate/jsvi

Structural intensity in plates with multiple discrete and distributed spring–dashpot systems

M.S. Khun[a], H.P. Lee[b,*], S.P. Lim[a]

[a] *Department of Mechanical Engineering, National University of Singapore, 9 Engineering Drive 1, 117576 Singapore*
[b] *Institute of High Performance Computing, 1 Science Park Road, #01-01 The Capricorn, Singapore Science Park II, 117528 Singapore*

Received 17 February 2003; accepted 6 August 2003

Abstract

The finite element method has been used to predict the structural intensity of a plate with multiple discrete and distributed dampers. Different combinations of dampers in different positions were employed to study the effects of multiple dampers in an individual plate model to examine the energy flow phenomenon in the presence of many dissipative elements. The structural intensity of plate structures connected by loosened bolts subjected to forced excitation is also presented in this paper. The loosened bolts are modelled by discrete as well as distributed spring–dashpot systems. The distributed springs and dampers are introduced to characterize the joint behavior of the plates. Numerical results are also presented for the plates connected by two bolts.

1. Introduction

A great attention has to be paid to the effects of dynamic loading on engineering structures. Structure-borne sound is associated with the vibrational energy which results from dynamically loaded mechanical and structural systems. This vibratory energy travelling along the structures is usually radiated as noise. In order to control vibration and structure-borne sound problems, the understanding of the behavior of a structure is desired. The structural intensity technique is a convenient way to describe the behavior of a structure.

The structural intensity fields indicate the magnitude and direction of energy flows in structural vibration at any point in a structure. Structural intensity vectors express the energy transmission

*Corresponding author. Tel.: +65-6419-1467; fax: +65-6419-1480.
E-mail address: hplee@ihpc.nus.edu.sg (H.P. Lee).

0022-460X/$ - see front matter
doi:10.1016/j.jsv.2003.08.002

paths and they also indicate the vibration source and energy sinks. The structural intensity was first introduced by Noiseux [1] and later developed by Pavic [2] and Verheij [3]. These works were mainly related to the experimental methods. Pavic [2] proposed a method for measuring the power flow due to flexural waves in beam and plate structures by using multiple transducers and digital processing techniques. Cross-spectral density methods were presented by Verheij [3] to measure structural power flow in beams and pipes. Pavic [4] proposed structural surface intensity measurements to analyze a more general vibration type and a structure with complicated geometry.

Computation of the structural intensity using the finite element method was developed by Hambric [5]. Not only flexural but also torsional and axial power flows were taken into account in calculating the structural intensity of a cantilever plate with stiffeners.

Pavic and Gavric [6] evaluated the structural intensity fields of a simply supported plate by using the finite element method. Normal mode summations and swept static solutions were employed for computing the structural intensity fields and identifying the source and the sinks of energy. The use of this modal superposition method was further extended to an experimental method by Gavric et al. [7]. Measurements were performed on a test structure consisting of two plates and the structure intensity was computed.

Li and Li [8] calculated the surface mobility for a thin plate by using structural intensity approach. The structural intensity fields of plates with viscous dampers and structural damping were computed using finite element analysis. The first effort to use solid finite elements to compute structural power flow was performed by Hambric and Szwerc [9] in a T-beam model. Measurements of structural intensity using optical methods were discussed in Refs. [10,11]. A z-shape beam was used in order to analyze the propagation of all types of waves in measuring structural intensity [10]. A laser Doppler vibrometer was employed to measure vibration velocities of the beam. Pascal et al. [11] presented the holographic interferometry method to obtain the phase and magnitude of the velocities of beams and plates. The structural intensity of a square plate with two excitation forces was calculated in the wave number domain and divergence of intensity was used to find out the position of the excitation points. Rook and Singh [12] studied the structural intensity of a bearing joint connecting a plate and a beam.

The damping capacities of joints play important roles in the analysis of the dynamic behavior of structures. Earles [13] estimated energy dissipation in a lap joint theoretically and concluded that it could attain comparable amounts of energy dissipation similar to that of using viscoelastic materials. Beard and Imam [14] studied the interfacial frictional forces of laminated plates to reduce the structural response and showed that the damping capacity was dependant on the clamping forces. Shin et al. [15] carried out experimental work on bolted joints for plate and shell structures and showed that the reduction in the contact pressure at the interface can maximize the energy dissipation at the joint. Beards and Woowat [16] analyzed the frictional damping caused by interfacial slip in a frame joint. It has been shown that both the amplitudes of response and frequencies at resonance could be altered by the clamping force.

The characteristics of a joint have been approximated with the use of spring–dashpot systems [17–20]. Amabili et al. [17] investigated a circular plate with elastic constraints at the free edges with artificial springs and applied this concept to bolted or riveted plates. A simplified joint model was proposed by Yoshimura and Okushima [18] and they developed a method to identify the stiffness and damping coefficients of the joint. Wang and Sas [19] presented an iteration method to

identify the parameters of a bolted joint by interactive use of experimental and simulation results. A lap jointed beam with two bolts was analyzed by Estenban et al. [20] at high frequencies and the energy dissipation at the joint was characterized by using both linear and non-linear models.

In this study, the structural intensity fields in plates are estimated by the use of the finite element method. Discrete dampers placed at various locations on a plate are preliminarily studied in order to examine the effects of multiple dampers. Two or more viscous dampers could be imagined as any two dissipative elements or causes of energy dissipation.

Simplified models consisting of springs and dampers are assumed to represent the characteristics of the bolted joint. Comparisons of the numerical results between the joint model comprised of single-point-type connections at bolt centers and the model with distributed connections around the bolted area on the joint are presented and discussed. The parameters of the bolts with the same clamping pressures are identified by iteration procedures. There are no reported works on the use of structural intensity to illustrate the flow of energy from the source to the point of energy dissipation at the joint-structure. The aim of this paper is to apply the structural intensity technique to analyze the energy dissipation of the bolted joints at junctions of the plates with a view of identifying such loosened joints in actual structures.

2. Computational methods

2.1. Formulation of structural intensity in a plate

Structural intensity is the power flow per unit area and it is analogous to acoustic intensity in a fluid medium. The time-averaged structural intensity nth component is defined as [6]

$$I_n(t) = -\sum_l \langle \sigma_{nl}(t) v_l(t) \rangle_t, \quad n, l = 1, 2, 3.$$

The n direction of active structural intensity inside an elastic medium in a frequency domain is given by [7]

$$I_n = -\tfrac{1}{2}\,\mathrm{Re}(\tilde{\sigma}_{nl}\tilde{v}_l^*), \quad n, l = 1, 2, 3,$$

where $\tilde{\sigma}$ is the complex amplitude of stress, $\tilde{v}_l^*$ is the complex conjugate of the velocity, and $\sim$ signs represent complex quantities.

Stresses and displacements are usually determined as stress results and movements of the mid-surface. Therefore, structural intensity in plates and shells are expressed in the form of power flow per unit width. Besides flexural deformations of the plate, the membrane effect is also considered in the formulation of structural intensity for shell elements. The x and y components of structural intensity for a flat plate using finite shell elements can be expressed as

$$I_x = -(\omega/2)\,\mathrm{Im}[\tilde{N}_x\tilde{u}^* + \tilde{N}_{xy}\tilde{v}^* + \tilde{Q}_x\tilde{w}^* + \tilde{M}_x\tilde{\theta}_y^* - \tilde{M}_{xy}\tilde{\theta}_x^*],$$

$$I_y = -(\omega/2)\,\mathrm{Im}[\tilde{N}_v\tilde{v}^* + \tilde{N}_{yx}\tilde{u}^* + \tilde{Q}_y\tilde{w}^* + \tilde{M}_y\tilde{\theta}_x^* - \tilde{M}_{yx}\tilde{\theta}_y^*],$$

where $\tilde{N}_x$, $\tilde{N}_y$ and $\tilde{N}_{xy} = \tilde{N}_{yx}$ are complex membrane forces per unit width of the plate; $\tilde{M}_x$, $\tilde{M}_y$ and $\tilde{M}_{xy} = \tilde{M}_{yx}$ are complex bending and twisting moments per unit width of the plate; $\tilde{Q}_x$ and $\tilde{Q}_y$ are complex transverse shear forces per unit width of the plate; $\tilde{u}^*$, $\tilde{v}^*$, and $\tilde{w}^*$ are complex

conjugate of translational displacements in the x, y and z directions; and $\tilde{\theta}_x^*$ and $\tilde{\theta}_y^*$ are complex conjugates of the rotational displacement about the x and y directions.

Power injected into a system is computed by multiplying input forces by the in phase components of the resulting velocities at the load points. The total input power due to point excitation forces can be calculated as [5]

$$P_I = \tfrac{1}{2}\,\Re\left[\sum_{i=1}^{n} \tilde{F}_i \tilde{v}_i^*\right],$$

where F_i corresponds to load and n is the number of loads.

The power output for a system is the power dissipating through the dampers and transmitting to the connecting systems such as spring or mass elements can be calculated by [5]

$$P_O = \tfrac{1}{2}\,\Re\left[\sum_{j=1}^{n} \tilde{F}_j \tilde{v}_j^*\right],$$

where F_j corresponds to the force of constraint and n is number of attached points.

2.2. The finite element analysis

Finite element computations in structural intensity were reported in Refs. [5–7]. Different finite element analysis software packages were applied for calculating the field variables of the model. The commercial FEM code NASTRAN was employed in the works [5,9]. The calculations in Ref. [8] were carried out by using the FEM software ANSYS. The commercial finite element analysis code ABAQUS [21] was used for all the calculations in this study.

The steady state dynamic analysis procedure was employed to obtain the magnitude and phase angle of the response of a harmonically excited system. ABAQUS provides the responses of structures in complex forms. The calculation of steady state harmonic response is not based on the modal superposition but is directly computed from the mass, damping and stiffness matrices of the model. Though it is more expensive in terms of computation, it can give more accurate results since it does not have error due to modal truncations.

2.3. Comparison of the results of the structural intensity for a plate with a damper

In this study, the structural intensity of a plate due to a point excitation force and an attached damper has been calculated using direct-solution steady state dynamic analysis. The results are then examined closely by comparing the computed structural intensity with the simulation data found in the published results. The result from Gavric and Pavic [6] using normal mode superposition with a swept-static term was selected to study the validity of numerical results computed by direct-solution steady state dynamic analysis. The same geometrical setup, boundary conditions, excitation frequency, material properties and loading conditions from the simulation carried out in Ref. [6] was used.

A steel plate, which was 3 m long, 1.7 wide and with the thickness of 1 cm, was used as the example problem [6]. The plate was simply supported. The material properties were as follows: Young's modulus = 210 GPa, the Poisson ratio = 0.3 and mass density = 7800 kg/m^3. The plate

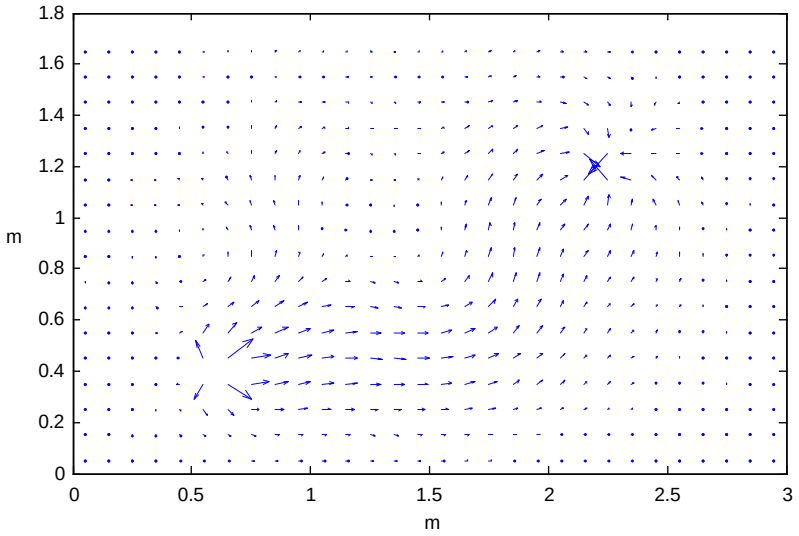

Fig. 1. The structural intensity field of a single steel plate with a point excitation force and an attached damper.

was assumed to be with no structural damping. The plate was modelled using 510 eight-node isoparametric shell element with 1625 nodes. The excitation force having a magnitude 1000 N with frequency of 50 Hz was applied at $x_f = 0.6$ m and $y_f = 0.4$ m on the plate. A dashpot element with a coefficient of damping of 100 N s/m was attached at the point $x_d = 2.2$ m and $y_d = 1.2$ m. The result of the simulation is shown in Fig. 1.

From the plot of the structural intensity vectors obtained by using direct steady state solution dynamic analysis, it can be seen that the structural intensity vectors indicate energy flows from the excitation point (energy source) to the damper (energy sink). This is consistent with the definition of structural intensity. This result is then compared with the results presented by Gavric and Pavic [6]. The comparison shows that the present results agree quite well with the published result. Furthermore, the result also validates that the direct solution steady state dynamic analysis is able to generate accurate results for the computation of structural intensity.

3. The structural intensity of a plate with multiple dampers

In order to investigate the parameters which may affect the energy flow of a plate structure with the same material properties and boundary conditions, the effects of the number of dampers, variations in damping coefficients, and positions of dampers and frequency are analyzed. Firstly, three simulations are carried out by attaching a dashpot having damping coefficient of 100 N s/m to the three positions, shown in Fig. 2, in turn at the excitation frequency of 17.36 Hz. The input and dissipated power balance are also carried out to validate the results. These simulations verify that these points are appropriate positions to which dampers are attached since the indications of source and sink are clear for all cases.

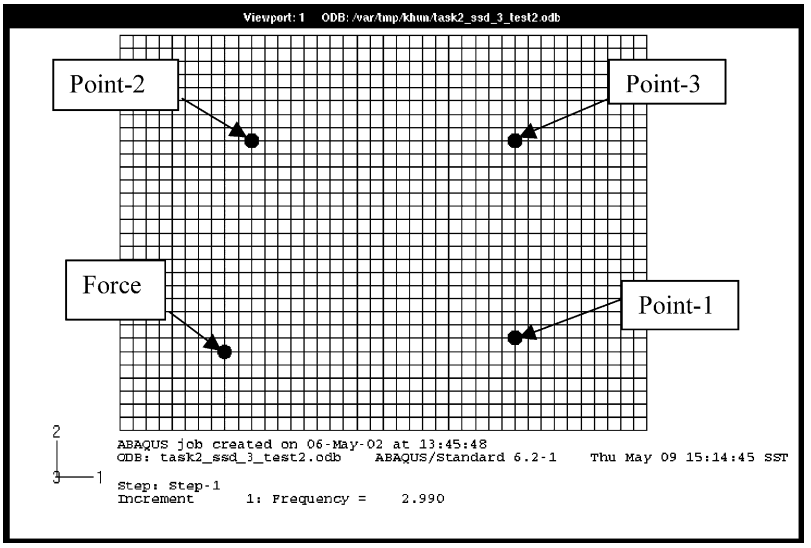

Fig. 2. The finite element model of plate showing positions of force and dashpots.

3.1. The finite element model used for multiple dampers

A steel plate was modelled using shell elements to study the effects of multiple dampers on the structural intensity in plate structures. Dimensions of the model are 2 m long, 1.5 m wide and 5 mm thick. The material properties are: Young's modulus (E) = 200 GPa, the Poisson ratio (v) = 0.3 and mass density (ρ) = 7800 kg/m^3. The excitation force having an amplitude of 10 N is applied at the lower left region ($x = 0.4$ m and $y = 0.3$ m). The plate is simply supported along its short edges. The plate is assumed to be with no structural damping. The plate is modelled using 1200 eight-node thick shell elements with reduced integration points having 3741 nodes.

Three positions shown in the finite element model (Fig. 2) were chosen as the attached points for two dashpots. The co-ordinates of these points are: $x = 1.5$ m, $y = 0.35$ m for the first point, $x = 0.5$ m, $y = 1.1$ m for the second point and $x = 1.5$ m, $y = 1.1$ m for the third point, respectively.

3.2. The effects of excitation frequency

The plate was excited at two low frequencies, 8.35 and 17.36 Hz to examine whether there were differences due to frequency on the intensity vectors. The above frequencies are near the first and the second resonance. By comparing Figs. 3 and 4, it indicates that there is a slight difference in the energy flow patterns between the two frequencies. The power flow path of the second is in a "U" shape pattern and propagates more broadly into the upper portion of the plate.

The influence of frequency on the effects of relative damping (discussed in the next section) was also examined. Parameters and positions of the dashpots were kept the same while the frequency was varied. The ratios of energy dissipation at individual dampers to the total dissipated energy are given in Tables 1 and 2. Comparison of the results in these two tables clearly indicates that they are of the same nature.

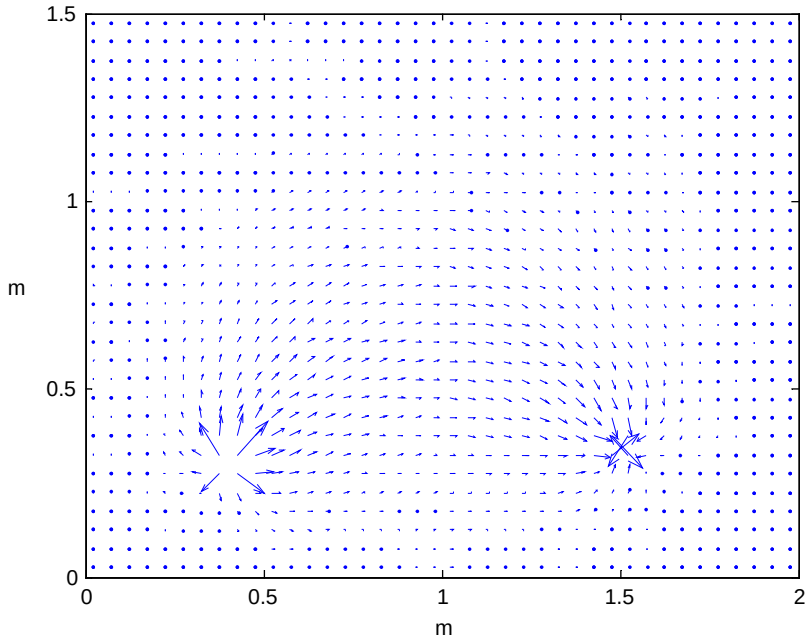

Fig. 3. Dashpot with damping coefficient of 100 N s/m at point-1; excitation frequency 8.35 Hz.

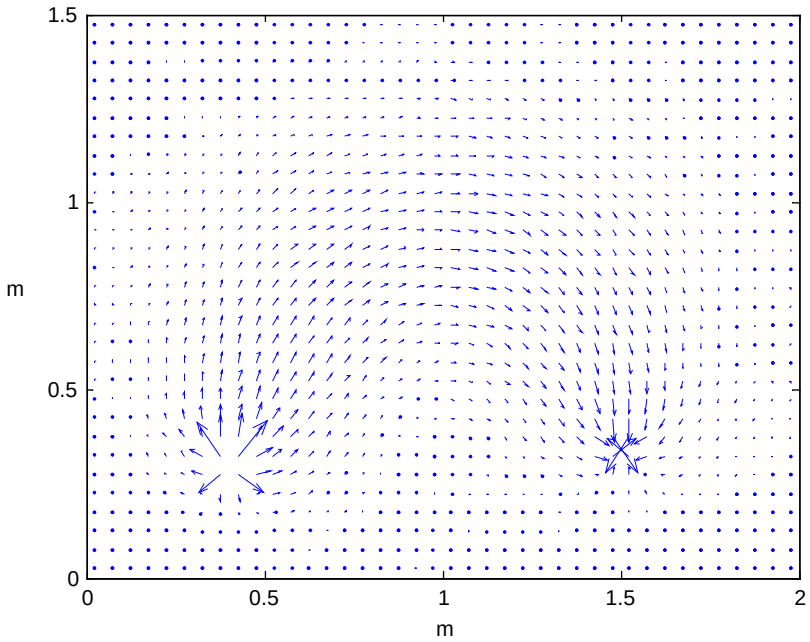

Fig. 4. Dashpot with damping coefficient of 100 N s/m at point-1; excitation frequency 17.36 Hz.

Table 1
Percentage of dissipated energy in a plate with multiple dampers at the frequency near the first resonance (8.35 Hz)

Damper point	Corresponding damping coefficients	Dissipated energy (%)
1,2	100,100	44.76–55.24
2,3	100,100	50.04–49.96
1,3	100,100	44.78–55.22
1,2	100,1000	7.76–92.24
2,3	1000,100	90.63–9.31
1,3	1000,100	88.76–11.24
1,2	100,20	80.19–19.81
1,2	15,20	37.83–62.17

Table 2
Percentage of dissipated energy in a plate with multiple dampers at the frequency near the second resonance (17.36 Hz)

Damper point	Corresponding damping coefficients	Dissipated energy (%)	Remark
1,2	100, 100	44.78–55.22	Fig. 5
2,3	100, 100	49.91–50.09	Fig. 6
1,3	100, 100	44.72–52.28	Fig. 7
1,2	100, 1000	8.73–91.63	Fig. 8
2,3	1000, 100	88.38–11.62	Fig. 9
1,3	1000, 100	85.70–14.3	Fig. 10
1,2	100, 20	80.19–19.91	
1,2	15, 20	37.84–62.16	

3.3. The effects of relative damping

In this case, two dampers were attached at two of the three allocated points in order to study the effects of two dampers at the forcing frequency of 17.36 Hz. Firstly, the dashpots with equal damping coefficient were employed. The damping coefficient of each dashpot was 100 N s/m. The locations of the two dampers were also changed to study the effect of the damper with respect to different positions. Figs. 5–7 show results from three combinations of positioning of the dampers. It can be observed from the above figures that dampers with equal damping capacity result in almost equal amounts of dissipation in the structural intensity diagrams.

Next, two dashpots having different damping coefficients were attached to the plate to investigate the effects of the relative damping capacities of dashpots on the structural intensity. One damper had a damping coefficient of 100 N s/m and the other had 1000 N s/m forming a ratio of 1:10 in damping coefficient. The results of three simulations at 17.36 Hz are shown in Figs. 8–10. The details of positions of dampers, damping coefficients and the ratios of the dissipated energy at these points to the total dissipated energy are given in Table 2 and the corresponding diagrams.

The energy sinks due to the larger dampers are obvious and the energy dissipations caused by lighter dampers cannot be seen clearly in the structural intensity vectors diagrams. It is more

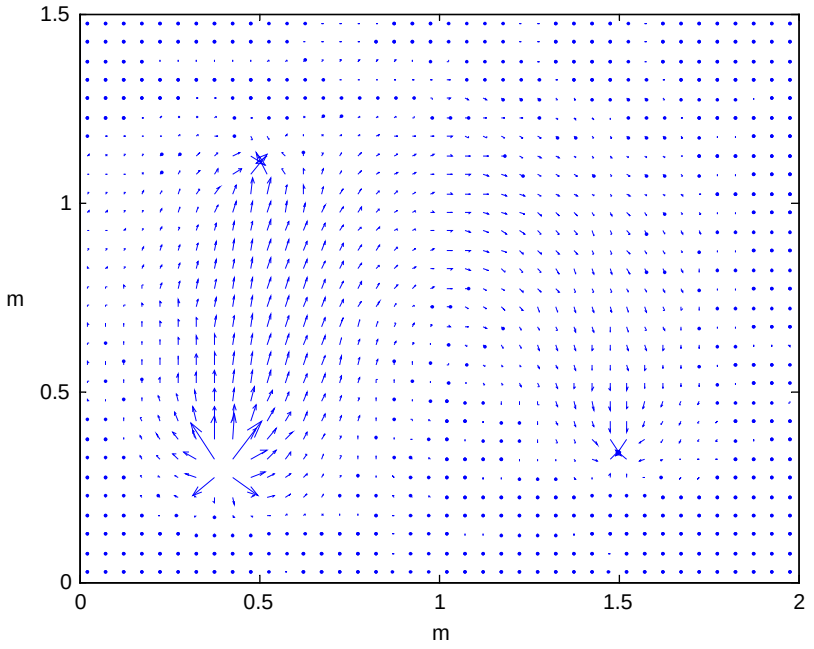

Fig. 5. Two dampers are attached at point-1 and point-2; damping coefficient 100 N s/m each; excitation frequency 17.36 Hz.

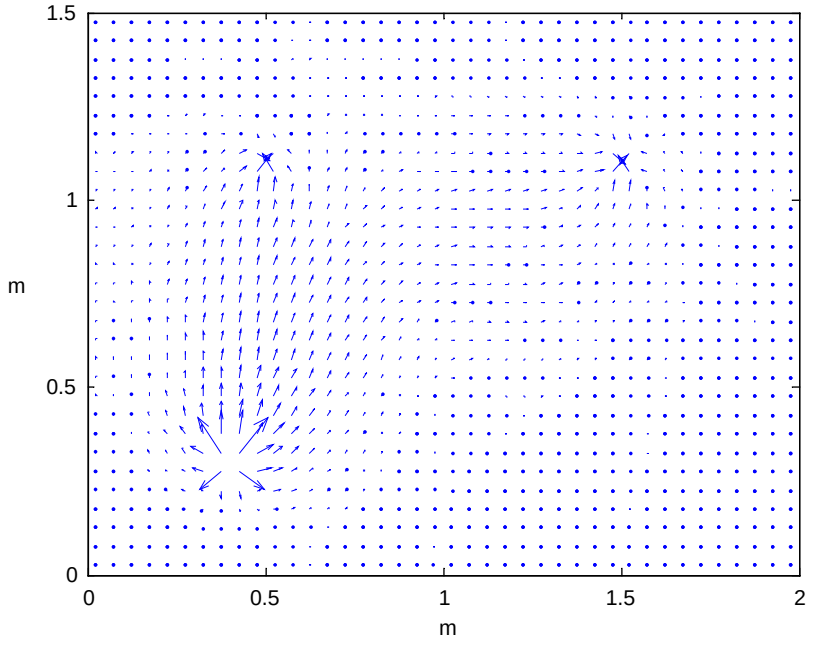

Fig. 6. Two dampers are attached at point-2 and point-3; damping coefficient 100 N s/m each; excitation frequency 17.36 Hz.

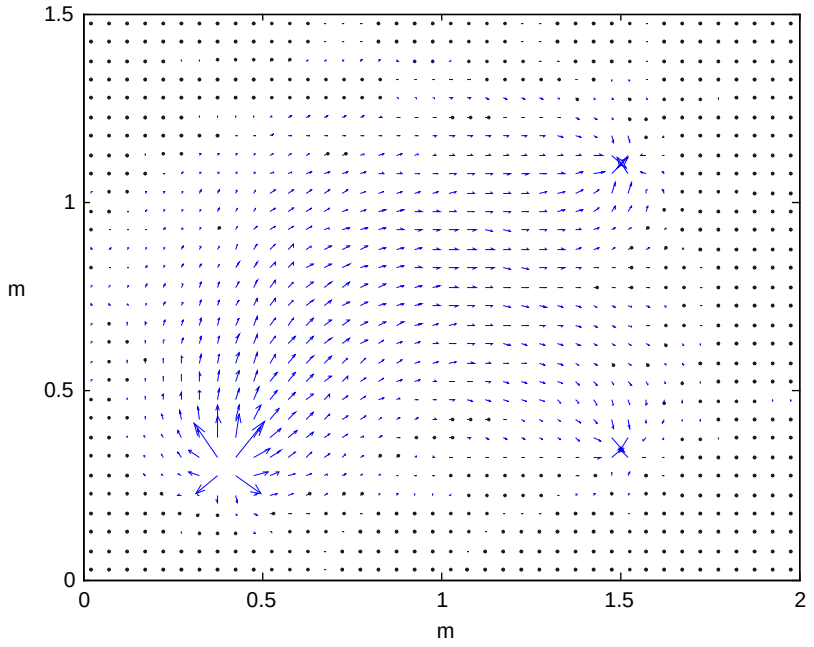

Fig. 7. Two dampers are attached at point-1 and point-3; damping coefficient 100 N s/m each; excitation frequency 17.36 Hz.

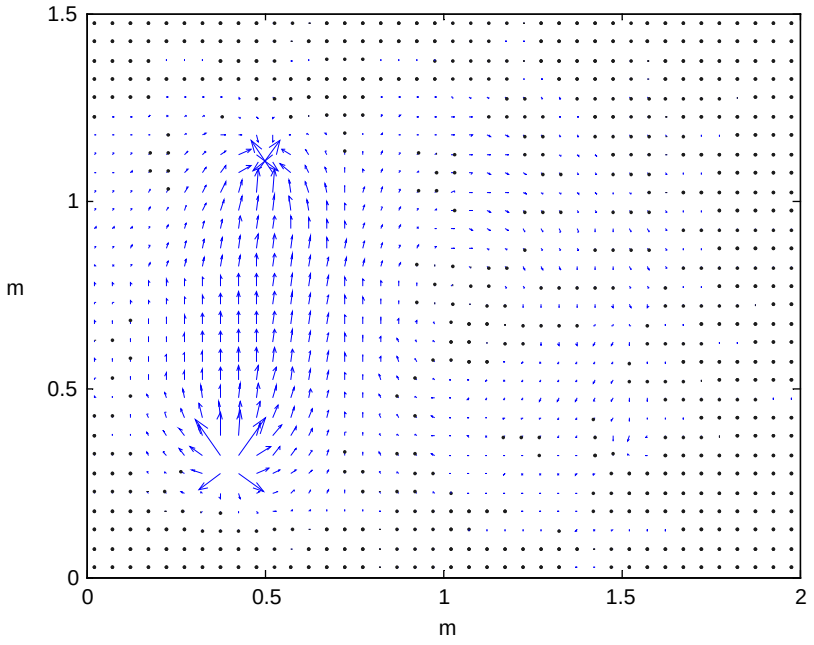

Fig. 8. A damper at point-2, damping coefficient 1000 N s/m; next damper at point-1, damping coefficient 100 N s/m; excitation frequency 17.36 Hz.

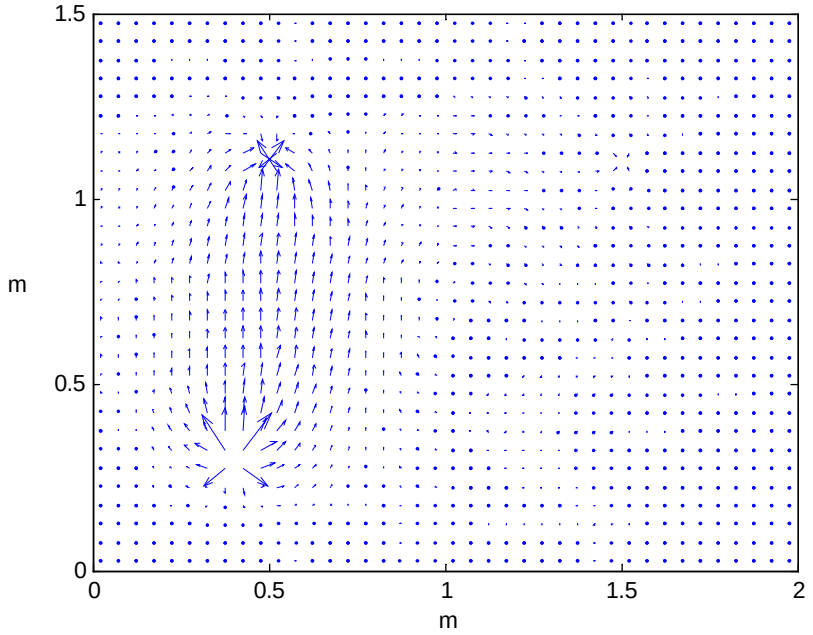

Fig. 9. A damper at point-2, damping coefficient 1000 N s/m; next damper at point-3, damping coefficient 100 N s/m; excitation frequency 17.36 Hz.

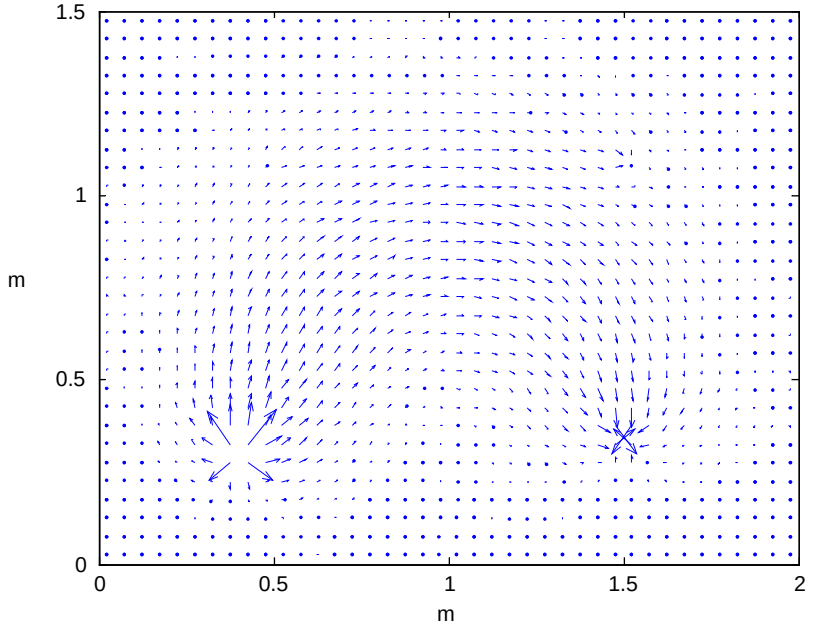

Fig. 10. A damper at point-1, damping coefficient 1000 N s/m; next damper at point-3, damping coefficient 100 N s/m; excitation frequency 17.36 Hz.

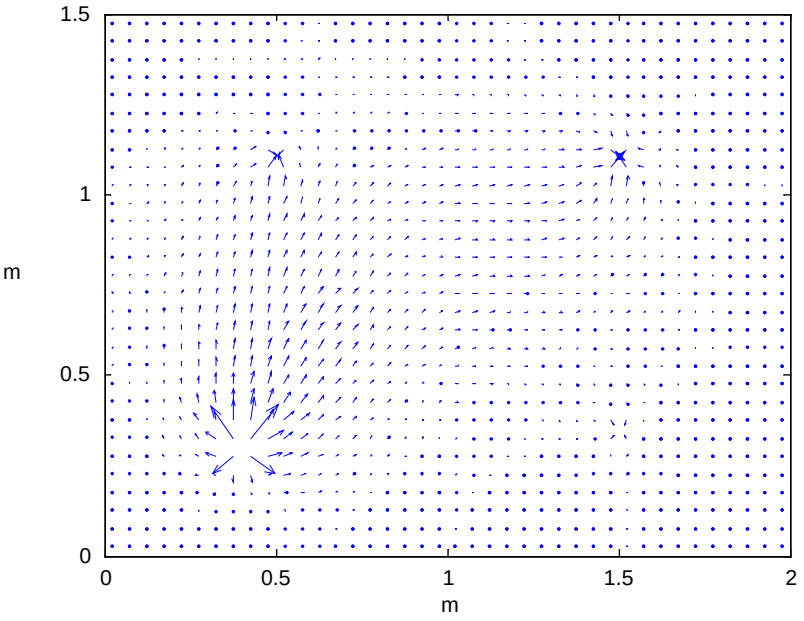

Fig. 11. Three dampers with different damping capacity at the excitation frequency of 17.36 Hz; the first damper at point-1 with damping coefficient of 200 N s/m; the second damper at point-2 with damping coefficient of 400 N s/m; the third damper at point-3 with damping coefficient 600 N s/m.

Table 3
Percentage of dissipated energy at three dampers (17.36 Hz)

Damper points	Corresponding damping coefficients	Dissipated energy ratio (%)	Remark
1,2,3	100, 200, 300	13.66, 34.22, 52.12	
1,2,3	200, 400, 600	12.92, 33.72, 53.36	Fig. 11
1,2,3	100 , 500, 1000	4.74, 29.58, 65.68	

significant when the greater energy dissipation occurs before the lower energy dissipation point along the energy flow path as in Fig. 8. These results imply that the structural intensity can reveal the relative energy dissipation at the dashpots.

These effects were further extended by examining two dashpots having different damping capacities but smaller coefficients of damping (100, 20 and 15, 20 N s/m). The energy ratios are given in Table 2 and they have the same behaviors. According to these results, the relative damping or the ratios of damping coefficients and the initial energy flow patterns are important in considering the positions to control the energy flow in a structure. Three dashpots with different coefficients are also considered and one of the results is shown in Fig. 11 and the energy ratios are given in Table 3.

4. Modelling of loosened bolts

4.1. Modelling the energy dissipated in loosened bolts

It has been discussed by many researchers [13–20] that most of the vibrational energy dissipation in built-up structures occurs at the joints. The mechanical joints are usually friction joints and the energy dissipation occurs when there is relative motion between the surfaces of the joint members and it results in energy loss of the whole system. It has been shown that the resonance frequencies and the energy dissipation arising from a joint are influenced by the clamping force on the mating section [13–16]. The clamping pressure on the joint can be controlled by adjusting applied torques on the bolts. When a bolt is loosened from firmly tightened by reducing the clamping force, relative motions exist between the mating surfaces and the macro-slip friction damping occurs in this region and it is assumed that Coulomb's law of friction holds [20].

The physical characteristics of a joint are non-linear and dependent on many conditions such as preloads on bolts, the coefficient of friction of surfaces, the amplitude and frequency of dynamic loading, temperature and many other factors. Non-linear behaviors of the joint and detailed contact problems are not taken into account in the present study in modelling the joint since the energy transmission and dissipation across a real joint is too complex to be treated computationally and analytically.

The dynamic rigidities and damping properties of the bolted joints can be estimated by equivalent linear spring–dashpot systems [17–20]. Springs maintain the appropriate rigidity for the joint connections and the viscous dampers provide the equivalent energy dissipation due to friction at the joint interfaces. These spring–dashpot models act in all six degrees of freedom (d.o.f.) of the shell elements.

In transverse vibration of a beam, the displacement d.o.f. of the joints associated with the excitation force can be reduced to two d.o.f., translation in the direction of force and rotation about the normal to the plane of force. The relative rotational displacements about the y-axis (γ direction) between joined nodes from each plate were dominant at the first bending mode and the rotational stiffness of the joint in this direction needs to restrict this rotation. Similarly, the relative translational displacements of these points in the z-direction were dominant at the second bending mode and the stiffness in this direction is also imposed to restrain these displacements. The relative displacements in all other directions were comparatively less than that of the predominant directions and springs in other directions were assumed to be rigid.

In this simulation, the lap joint of two plates is modelled by using the simple mathematical models consisting of parallel spring–dashpot systems positioned at the locations of the bolts. For the flexural vibration of plates, the stiffness in z and γ directions can be determined like those of beams. However, the unsymmetric location of the excitation force requires flexible stiffness in the α direction. Fortunately, the radial symmetric property of the bolt generally allows one to approximate the same parameters in two rotational directions, γ and α.

The coefficients of dashpots can also be approximated from the responses of these two modes using the half power point method [14,15]. The damping factors required for modelling the friction joint between the two plates were solved as the values from the model presented by Shin et al. [15]. The initial damping coefficients were assumed and then the responses for the range of

frequencies of interest could be found from simulations with appropriate frequency increments. The equivalent damping factors were measured from the plots for the frequencies against the response amplitudes. Comparisons between the acquired damping ratio and the damping ratio obtained from the published results were carried out. The procedures for estimating damping coefficients were repeated until a good agreement in the two damping factors was achieved.

4.2. The finite element model of plates with joints

The model for the present study consists of two square plates made of steel, connected by two bolts. The schematic diagram of the model indicating the positions of the bolts that fasten the two plates together and the position of the excitation force are shown in Fig. 12. The test structure is simply supported along its two short edges as shown in Fig. 13, the finite element model. The mesh densities near the bolts are increased as shown in Fig. 14. The radius of the circle around the center point is 0.025 m. Each plate has an area of 0.5 m × 0.5 m and a thickness of 5 mm. The material properties of the plates are as follows: Young's modulus is 210 GPa, the Poisson ratio is 0.3 and mass density is 7800 kg/m^3. The left hand side plate is subjected to a harmonic motion by a sinusoidal excitation force having a magnitude of 10 N and a frequency of 20.03 Hz. The excitation force is located in the left hand side of the plate at the coordinates of $x = 0.15$ m and $y = 0.15$ m. The plate–plate joint model is composed of 1056 eight-node shell elements and 3330 nodes. The positions of the upper bolt are $xa_1 = 0.45$ m and $ya_1 = 0.375$ m at the left hand side plate and $xb_1 = 0.05$ m and $yb_1 = 0.375$ m at the right hand plate. The locations of the lower bolts are $xa_2 = 0.45$ m and $ya_2 = 0.125$ m at the left plate and $xb_2 = 0.05$ m and $yb_2 = 0.125$ m at the right plate.

4.3. Identification of parameters

The joint was modelled in two manners. In the first case, the two plates were connected by the discrete spring–dashpot systems only at the center points of the circle as shown in Fig. 14(a). For the second case, the two plates were connected by the distributed spring–dashpot systems at all the

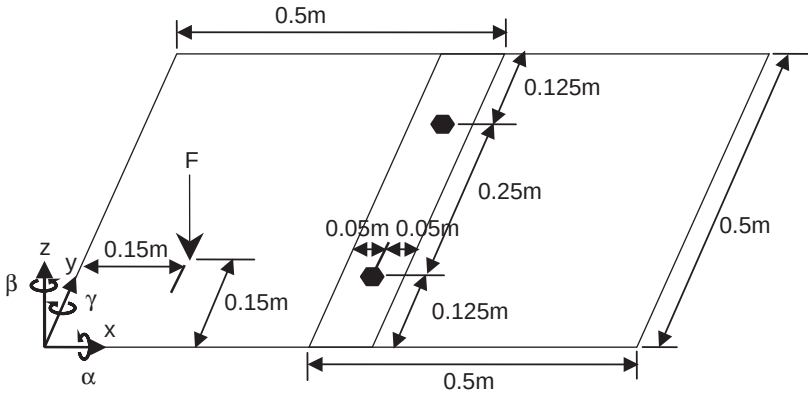

Fig. 12. Schematic diagram of two plates joined together by two bolts, showing the position of point excitation force and positions of the bolts on the plates.

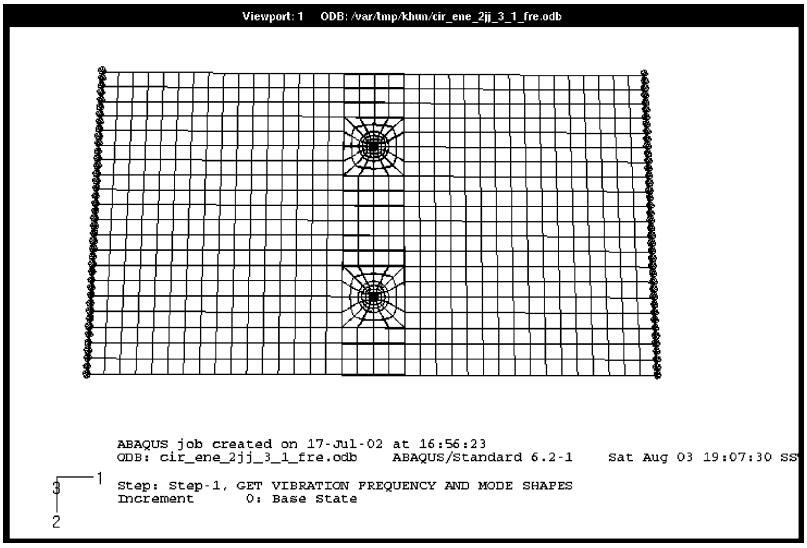

Fig. 13. The finite element model of plates overlap over a distance of 0.1 m.

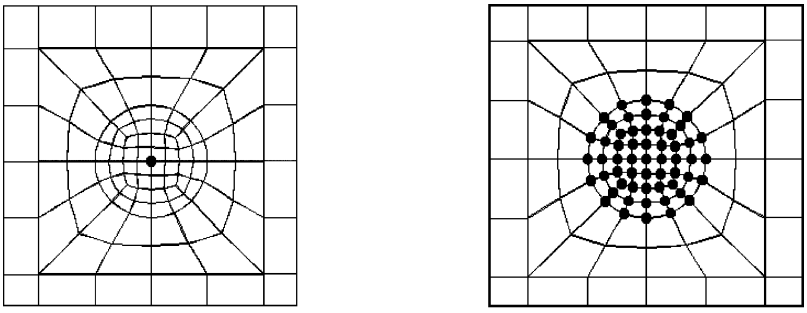

Fig. 14. (a) A spring–dashpot system connecting the two plates at the center point. (b) The distributed spring–dashpot systems connecting two plates over the finite circular area (solid circles show the positions of spring–dashpot systems).

corner nodes over the areas of the bolts as shown in Fig. 14(b) assuming that the clamping pressure was exerted over a finite area around the bolts. The physical parameters required for the finite element simulation were attained by using the procedures outlined above.

4.3.1. Single-point connected systems

The frequencies, 0.608 and 20.58 Hz, were selected as the resonance frequencies at the first and the second bending modes of the system attained from the experiment. The appropriate initial stiffness values for the springs were estimated first and the natural frequencies of the system were determined from simulations using ABAQUS [21], natural frequency extraction. The Lanczos method was used as the eigenvalue solver. Although the damping was present at the model, the natural frequencies of the system were approximated as the natural frequencies of the system are usually close to the resonance frequency with small damping.

When the two bolts are loosely tightened with the same torque so that the clamping pressure on the bolted areas on the plates are the same and the k and c values are, hence, taken to be the same for the springs and dashpots in the corresponding directions. The stiffness values and the corresponding coefficients of damping in all directions are listed in Table 4 and they were observed to be sufficiently rigid for supporting the structure.

4.3.2. Distributed spring–dashpot systems over a finite area

Since the shell element has little resistance against the drilling moment (normal to the shell), torsional springs with high stiffness and torsional dampers with large coefficients of damping usually causes localized rotational deformations around the attached points. In order to relieve the sudden increases in shear stresses associated with the localized rotational deformations, the distributed spring–dashpot systems were attached over circular areas to represent the bolts. The diameter of the outermost ring was 0.05 m. The pressures and the damping capacities were assumed to vary from the outermost ring to the inner rings linearly with a maximum at the center points. The values of the springs' stiffness and the damping coefficients were considered to be distributed in a similar manner.

The equivalent stiffness of the distributed springs was determined by comparing the frequencies of the present joint model to that of the previous joint model with a single spring–dashpot system. An iteration procedure was employed for estimating the stiffness. The damping coefficients of the distributed systems were calculated from single spring–dashpot systems in terms of the equivalent energy dissipation. The spring stiffness and damping coefficients of the distributed systems are listed in Tables 5 and 6.

Table 4
Spring stiffness and coefficients of dashpots for the single spring–dashpot system

Direction	Spring stiffness	Damping coefficient
Translation in $x(x)$	5.1×10^7 N/m	N/A
Translation in $y(y)$	5.2×10^7 N/m	N/A
Translation in $z(z)$	1.68×10^4 N/m	185 N s/m
Rotational about x (α)	2.98 N m/rad	0.0285 N m s/rad
Rotational about y (γ)	2.98 N m/rad	0.0285 N m s/rad
Rotational about z (β)	5 N m/rad	N/A

Table 5
Spring stiffness for distributed spring–dashpot systems

Direction	Units	Center	Ring 1	Ring 2	Ring 3	Ring 4
Translation in $x(x)$	N/m	5.1×10^6	4.1×10^6	3.1×10^6	2.1×10^6	1.1×10^6
Translation in $y(y)$	N/m	5.2×10^6	4.2×10^6	3.2×10^6	2.2×10^6	1.2×10^6
Translation in $z(z)$	N/m	4×10^3	4×10^2	3×10^2	2×10^2	1×10^2
Rotation about $x(\alpha)$	N m/rad	5×10^{-2}	4×10^{-2}	3×10^{-2}	2×10^{-2}	1×10^{-2}
Rotation about $y(\gamma)$	N m/rad	5×10^{-2}	4×10^{-2}	3×10^{-2}	2×10^{-2}	1×10^{-2}
Rotation about $z(\beta)$	N m/rad	5	4.5	3.6	2.2	1.5

Table 6
Damping coefficients for distributed spring–dashpot systems

Direction	Units	Center	Ring 1	Ring 2	Ring 3	Ring 4
Translation in z	N m/s	40.5	4.2	3.2	2.1	1.1
Rotation about x (α)	N ms/rad	7×10^{-4}	4×10^{-4}	3×10^{-4}	2×10^{-4}	1×10^{-4}
Rotation about y (γ)	N ms/rad	7×10^{-4}	4×10^{-4}	3×10^{-4}	2×10^{-4}	1×10^{-4}

5. Structural intensity of plates connected by loosened bolts

The structural intensities of the jointed structure with two joint models were computed for the frequency of second bending modes. The structural intensity fields are plotted for separate plates and the intensity vectors near the bolted regions are enlarged and shown next to the corresponding structural intensity diagrams of the plates.

5.1. Discrete connection

The structural intensity of the plates with single-point connections at the excitation frequency of 20.03 Hz, the second bending mode, is shown in Fig. 15. The positions of the energy sources and sinks can be identified for both plates and the energy flow paths are clear. Bolt positions are identified as the sinks for the excited plate. On the adjoining plate (right), the upper bolt acts as a source while the lower acts as a sink. In Fig. 15 b2, the intensity vectors are all entering the centre. The four vectors which appear to be emanating from the centre should be viewed as entering the center. The intensity near the centre is large and therefore causes the apparent visual misinterpretation. The main streams of energy flow in the plates are nearly a straight line from the source to the sink. It is clear from the fact that when the plate assembly is vibrating at it second bending mode, each plate resumes roughly the shape of its first bending mode. The main stream of power flow of a plate at its first bending mode and around this mode is nearly directly between the source and the sink (as in Fig. 3).

The total power exchange of the system between the force and the bolts can be obtained by two methods. The first method is the input power is directly computed from product of the input force and in-phase component of its velocity. The net power dissipated at the bolts is equal to the power dissipated at the dampers at the joint and it can also be calculated from the relative velocities across the dampers.

In the second manner, the power injected to the left plate by the excitation force is computed from integrating the structural intensity field by using the trapezoidal rule. Moreover, the amount of power leaving the first plate and entering and leaving the second plate can also be obtained from the integrated intensity around the bolts. The net energy loss at the upper bolt is the difference between the energy leaving the left plate and that entering the right plate. The sum of the energy leaving two plates at the lower bolt is equal to its total energy loss. Since there are no losses due to the structural damping, the power balance reveals the input power to the jointed plates system is nearly equal to the losses at the bolts for both methods. The input power of the whole assembly and power dissipated in the bolts are given in Tables 7 and 8. The results from the

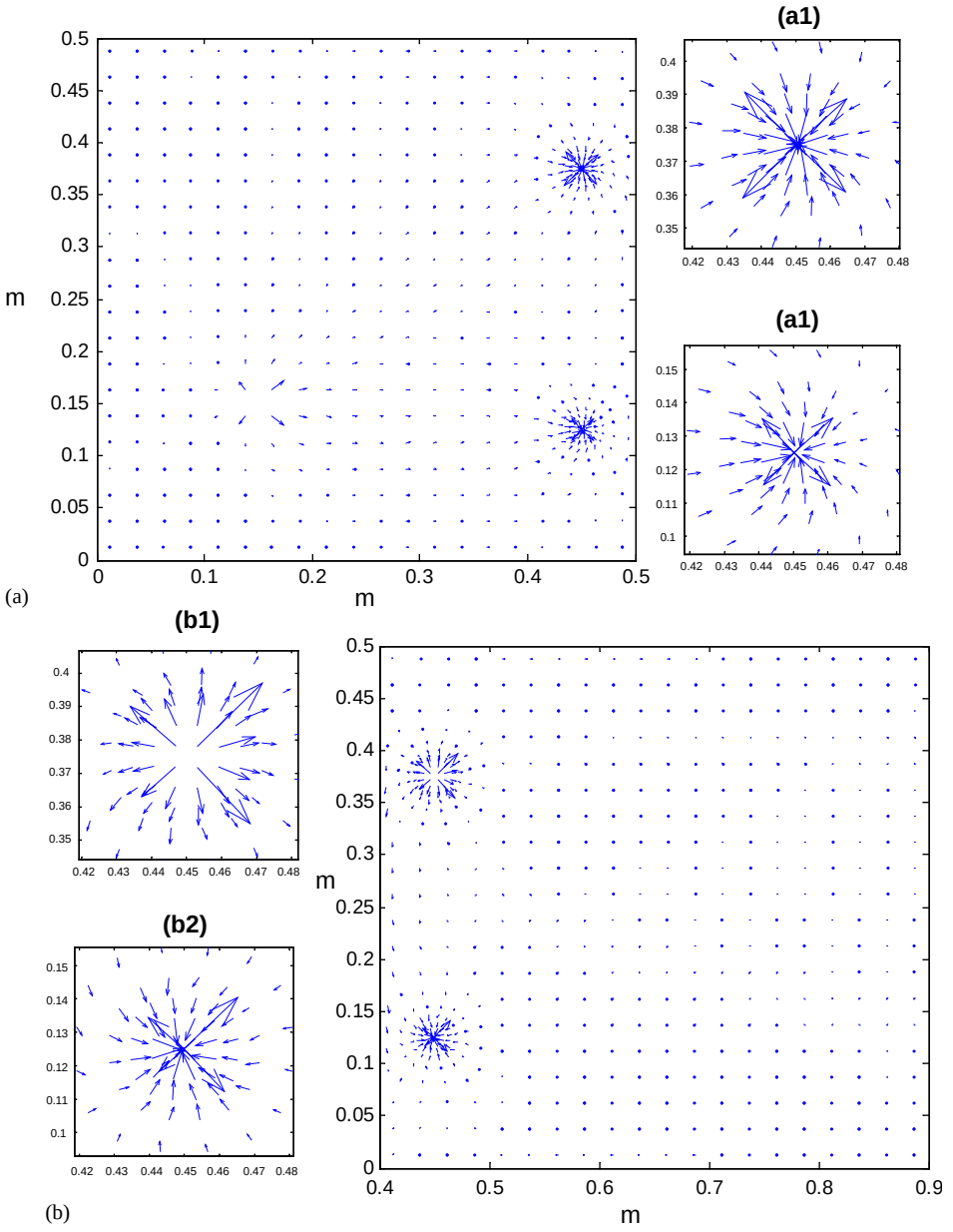

Fig. 15. Structural intensity of the plates with a single point attached spring–dashpots system. (a_1), (a_2), (b_2) and (b_1) show the enlarged views of the intensities near the bolts. Excitation frequency 20.03 Hz.

integration method are slightly greater than for the previous method. The slight errors between inputs and putouts are present in these results and it may be due to round off error involved in FEM analysis.

The energy dissipation and transmission characteristics of the joints can be interpreted from the intensities of plates. The transmission of energy from the first plate to the second plate can be

Table 7
Comparison of powers form velocity at 20.03 Hz

	Distributed systems	Discrete system
Input power (mW)	6.05	5.9
Total dissipated power (mW)	5.65	5.65
Lower bolt (mW)	3.4	3.45
Upper bolt (mW)	2.25	2.2
Percentage error of input to output (%)	6.6	4.2

Table 8
Comparison of powers from integration of SI at 20.03 Hz

	Distributed systems		Discrete system	
Input power (mW)	6.45		6.15	
Total dissipated power (mW)	6.45		6.2	
Power leaving and entering				
	Left plate	Right plate	Left plate	Right plate
Lower bolt (mW)	2.85 (out)	1.1 (out)	2.75 (out)	1.1 (out)
Upper bolt (mW)	3.6 (out)	1.1 (in)	3.45 (out)	1.1 (in)
Dissipated power				
Lower bolt (mW)	3.95		3.85	
Upper bolt (mW) in	2.6		2.45	
Percentage error of input to output (%)	0		0.08	

observed at the upper bolt. The transmitted energy is partially dissipated at this bolt but the excess energy becomes the energy input for the second plate. The energy dissipation characteristics of the joint can be clearly seen at the lower bolt. It acts as energy sinks by dissipating all the incoming energies from the two plates. These indications on the structural intensity diagrams agree well with the energy balance results in Tables 7 and 8. The unsymmetric position of the excitation force results in an unequal amount of energy flow across the joint and yields different energy losses in the bolts.

5.2. Distributed connection

Fig. 16 illustrates the structural intensity of plates with distributed systems and the intensity plots can describe the information of energy flow in the plates as well. The indications of intensity vectors are similar to that of the single-point connection systems except, the magnitudes of the

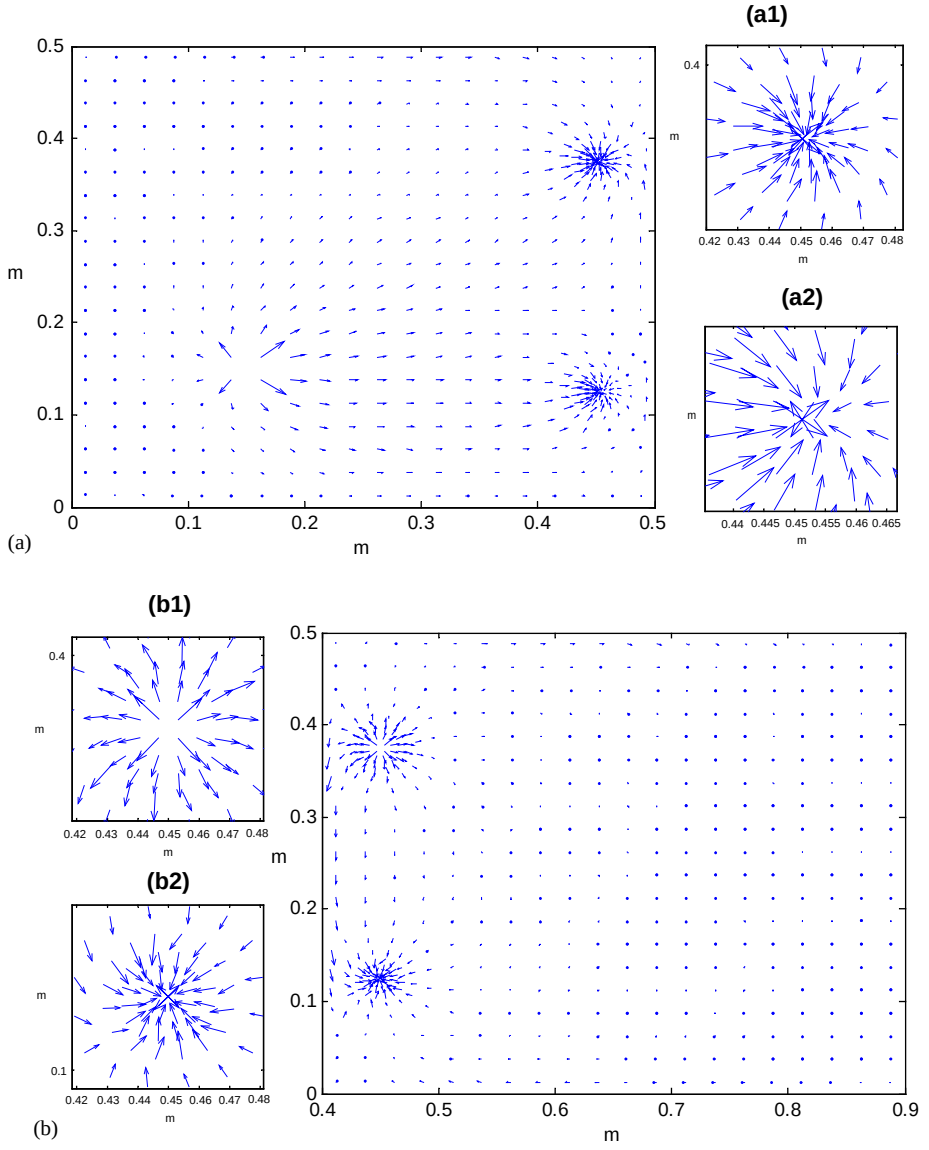

Fig. 16. Structural intensity fields of plates with distributed springs and dashpots systems. (a_1), (a_2), (b_1) and (b_2) show the enlarged views near the bolts. Excitation frequency 20.03 Hz.

intensity vectors at the center points are smaller. This is due to the fact that the energy dissipation occurs in distributed areas rather than at two points.

The results of energy balance for the distributed systems are listed in Tables 7 and 8. The amounts of injected power and total dissipated power are approximately the same for the former and the latter cases. Moreover, the power losses in the upper and the lower bolts are also nearly identical.

6. Conclusions

The structural intensity field provides the information of power flow and identifies the energy source and sinks for the plate structure with multiple dampers as well as for a single dashpot case. The power flow pattern and the amount of energy in a plate could be controlled by applying multiple dampers. In the presence of a damper with large damping coefficient, the next small damper has less effect in dissipating capability compared to the larger one. The structural intensities of the jointed plates can be estimated characterizing the energy transmission and dissipation of the loosened bolts at the joint using both discrete and distributed spring–dashpot systems. Good agreements in both the intensity diagrams and power balance are observed between the two models.

References

[1] D.U. Noiseux, Measurement of power flow in uniform beams and plates, *Journal of Acoustical Society of America* 47 (1970) 238–247.
[2] G. Pavic, Measurement of structure borne wave intensity, Part I: formulation of the methods, *Journal of Sound and Vibration* 49 (2) (1976) 221–230.
[3] J.W. Verheij, Cross-spectral density methods for measuring structure borne power flow on beams and pipes, *Journal of Sound and Vibration* 70 (1) (1980) 133–138.
[4] G. Pavic, Structural surface intensity: an alternative approach in vibration analysis and diagnosis, *Journal of Sound and Vibration* 115 (3) (1987) 405–422.
[5] S.A. Hambric, Power flow and mechanical intensity calculations in structural finite element analysis, *Journal of Vibration and Acoustics* 112 (1990) 542–549.
[6] L. Gavric, G. Pavic, A finite element method for computation of structural intensity by the normal mode approach, *Journal of Sound and Vibration* 164 (1) (1993) 29–43.
[7] L. Gavric, U. Carlsson, L. Feng, Measurement of structural intensity using a normal mode approach, *Journal of Sound and Vibration* 206 (1) (1997) 87–101.
[8] Y.J. Li, J.C.S. Lai, Prediction of surface mobility of a finite plate with uniform force excitation by structural intensity, *Applied Acoustics* 60 (2000) 371–383.
[9] S.A. Hambric, R.P. Szwerc, Prediction of structural intensity fields using solid finite element, *Noise Control Engineering Journal* 47 (1999) 209–217.
[10] A.A. Freschi, A.K.A. Pereira, K.M. Ahmida, J. Frejlich, J.R.F. Arruda, Analyzing the total structural intensity in beams using a homodyne laser doppler vibrometer, *Shock and Vibration* 7 (2000) 299–308.
[11] J.C. Pascal, X. Carniel, V. Chalvidan, P. Smigielski, Determination of phase and magnitude of vibration for energy flow measurements in a plate using holographic interferometry, *Optics and Lasers in Engineering* 25 (1996) 343–360.
[12] T.E. Rook, R.H. Singh, Structural intensity calculation for compliant plate-beam structures connected by bearings, *Journal of Sound and Vibration* 211 (3) (1998) 365–387.
[13] S.W.E. Earles, Theoretical estimation of the frictional energy dissipation in a simple lap joint, *Journal of Mechanical Engineering Science* 2 (1966) 207–214.
[14] C.F. Beards, I.M.A. Imam, The damping of plate vibration by interfacial slip between layers, *International Journal of Machine Tool Design and Research* 18 (1978) 131–137.
[15] Y.S. Shin, J.C. Iverson, K.S. Kim, Experimental studies on damping characteristics of bolted joints for plates and shells, *Journal of Pressure Vessel Technology* 113 (1991) 402–408.
[16] C.F. Beards, A. Woowat, The control of frame vibration by friction damping in joints, *Journal of Vibration, Acoustics, Stress, and Reliability in Design, Transactions of the American Society of Mechanical Engineers* 106 (1985) 26–31.

[17] M. Amabili, R. Pierandrei, G. Frosali, Analysis of vibrating circular plates having non-uniform constraints using the modal properties of free-edge plates: application to bolted plates, *Journal of Sound and Vibration* 206 (1) (1997) 23–38.
[18] M. Yoshimura, K. Okushima, Measurement of dynamic rigidity and damping property for simplified joint models and simulation by computer, *Annals of the CIRP* 25 (1977) 193–198.
[19] J. Wang, P. Sas, A method for identifying parameters of mechanical joints, *Journal of Applied Mechanics, Transactions of the American Society of Mechanical Engineers* 25 (1990) 337–342.
[20] J. Esteban, F. Lalande, Z. Chaudhry, C.A. Rogers, Theoretical modeling of wave propagation and energy dissipation in joints, *Proceedings of the 37th AIAA/ASME/ASCE/AHS/ASC Structures, Structural Dynamics, and Materials Conference*, Vol. AIAA#96-1278, 1996, pp. 131–141.
[21] *ABAQUS User's Manuals*, Version 6.2, Hibbitt, Karlsson and Sorensen, USA, 2001.